

The Performance of Space-Time Processing for Suppressing Narrowband Interference in CDMA Communications

A.M. HAIMOVICH and A. SHAH

Center for Communications and Signal Processing Research, Department of Electrical and Computer Engineering, New Jersey Institute of Technology, Newark, NJ 07102, U.S.A.

Abstract. The requirement to suppress narrowband interferences in CDMA communications stems from the overlay concept, i.e., coexistence of different types of signals in the same frequency band. The conventional approach to rejecting the narrowband interferences has been to whiten the received signal containing the interference, prior to spread spectrum demodulation. In this paper, it is proposed to achieve the interference rejection through spatial processing. The main benefit of this approach is its robustness with respect to the interference bandwidth. Stepping up from single domain spatial processing to space-time processing provides degrees of freedom for both overlay interference cancellation and diversity combining. Two space-time architectures, cascade and joint-domain, are studied and compared to a Rake receiver preceded by a whitening filter. Main contributions of the paper are the development of analytical expressions of (1) the efficiency of each method, (2) the p.d.f.'s of the output SNR in a Rayleigh fading environment, and (3) the error probability associated with each method. The analysis therein demonstrates that the joint-domain architecture outperforms the cascade configuration, which in turn is superior to the whitening filter-Rake combination.

Key words: smart antennas, narrowband interference rejection, space-time processing.

1. Introduction

The concept of an overlay has been proposed for both the PCS band [1] and the cellular band [2]. In such a scenario, DS CDMA signals are overlaid on top of existing narrowband users, providing new opportunities for the expansion of CDMA networks. In October 1993, the US Federal Communications Commission (FCC) released 140 MHz of spectrum in the 1.85 to 1.99 GHz region for use in PCS applications. The IS-95 direct-sequence (DS) CDMA has been proposed for use in the PCS frequency band. This PCS spectrum, however, is currently occupied by point-to-point, fixed service, relatively narrowband microwave radio links. The coexistence of these two different systems within the same frequency spectrum will cause interference to both systems. In this work we are concerned with the interference caused by the narrowband signal to the spread spectrum signal.

Starting with the days when spread spectrum was contemplated mainly for military communications, and the main concern were jammers intended to deny communications, and through recent work concerned with overlay of commercial applications, a considerable body of knowledge was generated on the topic of narrowband interference rejection in DS spread spectrum signals. The conventional approach was to sample the received signal at the chip interval, and to exploit the high correlation between the interference samples to whiten the signal prior to spread spectrum demodulation [3, 4]. This method essentially places a notch at the narrowband interference frequency. The notch, however, also removes a portion of the DS signal. As the bandwidth of the interference increases, the notch widens and the DS signal loss becomes more significant. In some CDMA applications the channel is frequency-selective and a receiver which consists of a whitening filter and a Rake combiner was proposed in [5].

More recent work exploited the binary nature structure of the DS signal to obtain improved interference rejection through nonlinear filtering [6]. When the narrowband interference is itself a DS sequence of a much lower rate, a multiuser framework was proposed for optimal interference rejection [7].

A different approach is the use of antenna arrays. Antenna arrays can provide diversity paths to combat multipath induced fading and are capable of suppressing interferences through spatial filtering [8]. The main advantage of spatial over temporal processing is in the bandwidth reference; in spatial processing the reference is the carrier frequency, while in temporal processing the reference is the bandwidth of the spread spectrum signal. With respect to the carrier frequency, even the spread spectrum signal is essentially narrowband. Thus, unlike the performance of the whitening filter, the spatial processor is very robust with respect to the interference bandwidth.

In this paper we consider the suppression of narrowband signals overlaid with the CDMA signal. A major source of interference in CDMA communications is the multiple access interference (MAI). Space-time receiver architectures have been previously proposed for MAI cancellation [9, 10, 11]. In this paper, these structures are evaluated for their performance in suppressing narrowband interferences. While the study of the overlay concept and the receivers investigated are motivated by CDMA communications, in this paper we focus on the rejection of narrowband interferences and ignore MAI effects. MAI cancellation in overlay situations is studied in [12].

The performance of adaptive antenna arrays in a Rayleigh fading channel has been studied in [13] and [8]. In those references it was shown that the interference cancellation entails a loss of degrees of freedom, with a corresponding loss in the diversity performance. In this paper, we demonstrate this suppression/diversity relation through an argument based on the asymptotic efficiency. Moreover, we extend the work in [13] and [8] by obtaining expressions for the probability density function (p.d.f.) of the SNR, and the error probability in a frequency-selective Rayleigh channel.

In section 2, we study interference suppression by way of single domain processing. The advantages of spatial processing are demonstrated by evaluation of the asymptotic efficiency for each method. In section 3, two space-time architectures, cascade space-time and joint-domain, are compared to the 'time-time' structure consisting of a prediction-error filter (PEF) and a Rake receiver (PEF-Rake), as proposed in [5]. Expressions for the SNR p.d.f. and the error probability are provided in section 4. Numerical results are presented in section 5, and conclusions are summarized in section 6.

2. Single Domain Processing

In this section, the signal model is introduced and the interference suppression processing is formulated in the temporal and spatial domains. Bandwidth effects are considered for each processing scheme.

SIGNAL MODEL

Consider the uplink of a coherent mobile communication system. The lowpass equivalent of the CDMA signal transmitted by a designated user is given by

$$s(t) = \sqrt{\mathcal{E}} \sum_i d(i) u(t - iT), \quad (1)$$

where \mathcal{E} is the symbol energy, $d(i) \in \{-1, 1\}$ is the data bit, T is the symbol interval, and $u(t)$ is a real-valued signature waveform¹ with unit energy $\int_0^T u^2(t) dt = 1$. The channel is assumed frequency-selective with M resolvable paths. Neglecting attenuation effects and assuming slow fading (unchanged over the processing interval), the received pulse shape is given by

$$\begin{aligned} g(t) &= \sum_{m=0}^{M-1} c_m u(t - mT_d) \\ &= \mathbf{c}^T \mathbf{u}(t), \end{aligned} \quad (2)$$

where the superscript (T) denotes transposition, c_m , $m = 0, \dots, M-1$, are the complex-valued channel coefficients, $\mathbf{c}^T = [c_0, \dots, c_{M-1}]$, and $\mathbf{u}(t)^T = [u(t), \dots, u(t - (M-1)T_d)]$. For a Rayleigh fading channel, c_m are modeled as independent identically distributed (i.i.d.) circular gaussian random variables with zero-mean and unity variance, i.e., $c_m \sim \text{CN}[0, 1]$. The tap-delay T_d , is chosen to model independent paths. In general, if the CDMA signal bandwidth is W , the bandwidth of the lowpass waveform $g(t)$ is $W/2$, the sampling frequency is W , and $T_d = 1/W$. In any specific application however, the signal may be received via few and widely dispersed paths, i.e., many of the coefficients of the model above may be set to zero.

The signal is received in the presence of narrowband interference and white gaussian noise. The interference is assumed to be a narrowband BPSK signal represented by the complex envelope

$$j(t) = \sqrt{J} b(t) e^{j(\Omega t + \theta_J)}, \quad (3)$$

where Ω is the offset between the carriers of the CDMA signal and the interference, $b(t)$ is a binary waveform with symbol interval T_j , J is the interference power, and θ_J is the interference carrier phase relative to the CDMA carrier. It is assumed that fading does not affect the narrowband interference. This assumption is of no great consequence, since given sufficient degrees of freedom, the interference is suppressed, whether fading or not. The interference fractional bandwidth is $p = T_c/T_j$. The noise $v(t)$ is a sample function of a gaussian complex-valued random process, with zero-mean and $E[|v(t)v^*(\tau)|] = N_o \delta(t - \tau)$. The received signal can then be written

$$r(t) = \sqrt{\mathcal{E}} \sum_i d(i) g(t - iT) + j(t) + v(t). \quad (4)$$

Two interference suppression schemes configurations, operating in the temporal and spatial domains, respectively, are considered below.

TEMPORAL INTERFERENCE SUPPRESSION

Temporal interference suppression is implemented by a PEF. Assuming that the filter tap-delay is the same as in the channel model, the output of the PEF can be written

$$x(t) = \sqrt{\mathcal{E}} \sum_i d(i) \mathbf{a}^H \mathbf{U}^T(t - iT) \mathbf{c} + \mathbf{a}^H \mathbf{j}_t(t) + \mathbf{a}^H \mathbf{v}_t(t), \quad (5)$$

¹ This model is not applicable to IS-95 since the signature is repeated at each symbol interval. This restriction is adopted only for notational convenience, and the results in the paper apply also for long codes.

where the superscript (H) denotes 'transpose-conjugate'. The filter coefficients are contained in the Q -dimensional vector \mathbf{a} , and the $M \times Q$ matrix $\mathbf{U}(t)$ is defined

$$\mathbf{U}(t) = [\mathbf{u}(t), \dots, \mathbf{u}(t - (Q - 1)T_d)]. \quad (6)$$

The interference vector is defined $\mathbf{j}_t^T(t) = [j(t), \dots, j(t - (Q - 1)T_d)]$, $\mathbf{v}_t(t)$ is defined in a similar manner, and the M -dimensional vector \mathbf{c}^T consists of the channel coefficients. Spread spectrum demodulation at the k -th data bit interval yields:

$$\begin{aligned} x(k) &= \langle x(t), u(t - kT) \rangle \\ &= d(k) \sqrt{\mathcal{E}} \mathbf{a}^H \mathbf{P}_0^T \mathbf{c} + d(k+1) \sqrt{\mathcal{E}} \mathbf{a}^H \mathbf{P}_1^T \mathbf{c} + \mathbf{a}^H \mathbf{j}_t(k) + \mathbf{a}^H \mathbf{v}_t(k), \end{aligned} \quad (7)$$

where $\langle x(t), u(t - kT) \rangle = \int_{kT}^{(k+1)T} x(t) u(t - kT) dt$, and

$$\mathbf{P}_\ell = \langle \mathbf{U}(t + \ell T), \mathbf{u}(t) \rangle \quad \ell = 0, 1 \quad (8)$$

is the $M \times Q$ spreading sequence correlation matrix. The interference vector is defined $\mathbf{j}_t(k) = \langle \mathbf{j}_t(t), u(t) \rangle$, and the noise vector $\mathbf{v}_t(k)$ is defined similarly. To facilitate the analysis, assume that the autocorrelation of the signature waveform is such that $[\mathbf{P}_0]_{11} = 1$ is the only non-zero element of the matrix \mathbf{P}_0 , and that $\mathbf{P}_1 = \mathbf{0}$. Since $\langle x(t), u(t - kT) \rangle = \mathbf{a}^H \langle \mathbf{r}(t), u(t - kT) \rangle \equiv \mathbf{a}^H \mathbf{r}(k)$, where $\mathbf{r}^T(t) = [r(t), \dots, r(t - (M - 1)T_d)]$, the demodulated signal across the filter taps is given by,

$$\mathbf{r}(k) = d(k) \sqrt{\mathcal{E}} c_0 \mathbf{e}_0 + \mathbf{j}_t(k) + \mathbf{v}_t(k), \quad (9)$$

where $\mathbf{e}_0^T = [1, 0, \dots, 0]$. It is well known that coefficients of the PEF are given by (see for example [14])

$$\mathbf{a} = \mathbf{R}_t^{-1} \mathbf{e}_0, \quad (10)$$

where the temporal correlation matrix is given by $\mathbf{R}_t = E [\mathbf{r}(k) \mathbf{r}^H(k)]$.

The *asymptotic efficiency* is defined as

$$\eta = \lim_{N_o \rightarrow 0} \frac{\text{SNR}_{\text{eff}}}{\text{SNR}}, \quad (11)$$

where SNR_{eff} is measured in the presence of the interference, and SNR is observed with the interference absent. This definition is restricted to the effect of the processing on the interference and it does not account for diversity combining. It can be interpreted as the efficiency of the processor in the sense of the relative number of degrees of freedom leftover after interference cancellation and available for other purposes (such as diversity combining). The asymptotic efficiency is used in this paper as a figure of merit.

In the case of a single tone interference, the asymptotic efficiency of the PEF can be evaluated analytically. With the interference absent, the output of the PEF is given by $U = \mathbf{e}_0^T \mathbf{r}(k) = d(k) \sqrt{\mathcal{E}} c_0 + v_{t0}(k)$, where $v_{t0}(k)$ is the first component of the noise vector $\mathbf{v}_t(k)$. It follows that,

$$\text{SNR} = \frac{|E[U]|^2}{\text{var}(U)} \quad (12)$$

$$= \frac{|c_0|^2 \mathcal{E}}{N_o}. \quad (13)$$

From Equation (3), for a single tone interference $j(t) = \sqrt{J}e^{j(\Omega t + \theta_J)}$. If $\Omega \ll 1/T$, we have $\langle j(t), u(t - kT) \rangle \simeq \sqrt{J'}e^{j(\Omega(k+1/2)T + \theta_J)}$, where $J' = J/G$ and G is the spread spectrum processing gain. The interference vector can then be written, $\mathbf{j}_t(k) = \langle \mathbf{j}_t(t), u(t) \rangle = \sqrt{J'}e^{j(\Omega(k+1/2)T + \theta_J)}\mathbf{f}_1$, where $\mathbf{f}_1^T = [1, e^{-j\Omega T_d}, \dots, e^{-j\Omega(Q-1)T_d}]$. The assumption is that $J \gg \mathcal{E}$ (otherwise there would be no need for the interference suppression filter). It follows that

$$\mathbf{R}_t = J'\mathbf{f}_1\mathbf{f}_1^H + (|c_0|^2\mathcal{E} + N_o)\mathbf{I}_Q, \quad (14)$$

where \mathbf{I}_Q is the Q -dimensional unity matrix. Letting $N_o \rightarrow 0$, $J' \gg |c_0|^2\mathcal{E}$, and using the matrix inversion lemma, it can be easily shown that \mathbf{a} in Equation (10) can be expressed (within a constant factor) as

$$\mathbf{a} = \mathbf{e}_0 - \frac{1}{Q}\mathbf{f}_1. \quad (15)$$

The SNR is invariant to the gain of the vector \mathbf{a} . It can be readily verified that $\mathbf{a}^H\mathbf{f}_1 = 0$, i.e., the tone interference is completely removed by the PEF. The output of the PEF is then given by $U_1 = \mathbf{a}^H\mathbf{r}(k) = d(k)\sqrt{\mathcal{E}}c_0\mathbf{a}^H\mathbf{e}_o + \mathbf{a}^H\mathbf{v}_t(k)$. Let $a_0 \equiv \mathbf{a}^H\mathbf{e}_o$, then $U_1 = d(k)\sqrt{\mathcal{E}}c_0a_0 + \mathbf{a}^H\mathbf{v}_t(k)$. We have,

$$\text{SNR}_{\text{eff}} = \frac{|a_0c_0|^2\mathcal{E}}{N_o\|\mathbf{a}\|^2}, \quad (16)$$

where $\|\mathbf{a}\|^2 \equiv \mathbf{a}^T\mathbf{a}$. From Equation (15) it follows that $\|\mathbf{a}\|^2 = \left(1 - \frac{1}{Q}\right)$ and $|a_0|^2 = \left(1 - \frac{1}{Q}\right)^2$. Hence,

$$\text{SNR}_{\text{eff}} = \frac{|c_0|^2\mathcal{E}}{N_o} \left(1 - \frac{1}{Q}\right) \quad (17)$$

From Equations (12) and (17), the asymptotic efficiency of the temporal processor for a tone interference is

$$\eta_t = 1 - \frac{1}{Q}. \quad (18)$$

This relation clearly demonstrates the loss of one degree of freedom incurred by the interference cancellation process. The spatial processor is considered next.

SPATIAL PROCESSING

Consider an N -element antenna array at the base station. Then using Equation (4), the signal received at the n -th antenna in the frequency-selective channel modeled by an M -tap delay line can be written,

$$r_n(t) = \sqrt{\mathcal{E}} \sum_i d(i)g_n(t - iT) + j_n(t) + v_n(t), \quad (19)$$

where $g_n(t) = \mathbf{c}_n^T\mathbf{u}(t)$, \mathbf{c}_n is the channel vector seen by the n th antenna, $j_n(t) = j(t)e^{j\psi_n}$, and the interference phase is ψ_n . The array elements are assumed sufficiently separated such

From Equation (3), for a single tone interference $j(t) = \sqrt{J}e^{j(\Omega t + \theta_J)}$. If $\Omega \ll 1/T$, we have $\langle j(t), u(t - kT) \rangle \simeq \sqrt{J'}e^{j(\Omega(k+1/2)T + \theta_J)}$, where $J' = J/G$ and G is the spread spectrum processing gain. The interference vector can then be written, $\mathbf{j}_t(k) = \langle \mathbf{j}_t(t), u(t) \rangle = \sqrt{J'}e^{j(\Omega(k+1/2)T + \theta_J)}\mathbf{f}_1^T$, where $\mathbf{f}_1^T = [1, e^{-j\Omega T_d}, \dots, e^{-j\Omega(Q-1)T_d}]$. The assumption is that $J \gg \mathcal{E}$ (otherwise there would be no need for the interference suppression filter). It follows that

$$\mathbf{R}_t = J'\mathbf{f}_1\mathbf{f}_1^H + (|c_0|^2\mathcal{E} + N_o)\mathbf{I}_Q, \quad (14)$$

where \mathbf{I}_Q is the Q -dimensional unity matrix. Letting $N_o \rightarrow 0$, $J' \gg |c_0|^2\mathcal{E}$, and using the matrix inversion lemma, it can be easily shown that \mathbf{a} in Equation (10) can be expressed (within a constant factor) as

$$\mathbf{a} = \mathbf{e}_0 - \frac{1}{Q}\mathbf{f}_1. \quad (15)$$

The SNR is invariant to the gain of the vector \mathbf{a} . It can be readily verified that $\mathbf{a}^H\mathbf{f}_1 = 0$, i.e., the tone interference is completely removed by the PEF. The output of the PEF is then given by $U_1 = \mathbf{a}^H\mathbf{r}(k) = d(k)\sqrt{\mathcal{E}}c_0\mathbf{a}^H\mathbf{e}_o + \mathbf{a}^H\mathbf{v}_t(k)$. Let $a_0 \equiv \mathbf{a}^H\mathbf{e}_o$, then $U_1 = d(k)\sqrt{\mathcal{E}}c_0a_0 + \mathbf{a}^H\mathbf{v}_t(k)$. We have,

$$\text{SNR}_{\text{eff}} = \frac{|a_0c_0|^2\mathcal{E}}{N_o\|\mathbf{a}\|^2}, \quad (16)$$

where $\|\mathbf{a}\|^2 \equiv \mathbf{a}^T\mathbf{a}$. From Equation (15) it follows that $\|\mathbf{a}\|^2 = \left(1 - \frac{1}{Q}\right)$ and $|a_0|^2 = \left(1 - \frac{1}{Q}\right)^2$. Hence,

$$\text{SNR}_{\text{eff}} = \frac{|c_0|^2\mathcal{E}}{N_o} \left(1 - \frac{1}{Q}\right) \quad (17)$$

From Equations (12) and (17), the asymptotic efficiency of the temporal processor for a tone interference is

$$\eta_t = 1 - \frac{1}{Q}. \quad (18)$$

This relation clearly demonstrates the loss of one degree of freedom incurred by the interference cancellation process. The spatial processor is considered next.

SPATIAL PROCESSING

Consider an N -element antenna array at the base station. Then using Equation (4), the signal received at the n -th antenna in the frequency-selective channel modeled by an M -tap delay line can be written,

$$r_n(t) = \sqrt{\mathcal{E}} \sum_i d(i)g_n(t - iT) + j_n(t) + v_n(t), \quad (19)$$

where $g_n(t) = \mathbf{c}_n^T\mathbf{u}(t)$, \mathbf{c}_n is the channel vector seen by the n th antenna, $j_n(t) = j(t)e^{j\psi_n}$, and the interference phase is ψ_n . The array elements are assumed sufficiently separated such

It follows,

$$\begin{aligned} \text{SNR}_{\text{eff}} &= \frac{\mathcal{E} |\omega_0^H \mathbf{k}_0|^2}{\frac{1}{2} N_o \|\omega_0\|^2} \\ &= \frac{\mathcal{E}}{\frac{1}{2} N_o} \mathbf{k}_0^H \left(\mathbf{I}_N - \frac{1}{N} \mathbf{g}_1 \mathbf{g}_1^H \right) \mathbf{k}_0. \end{aligned} \quad (27)$$

Since in the absence of interference, $\text{SNR} = \|\mathbf{k}_0\|^2 \mathcal{E} / \frac{1}{2} N_o$, the asymptotic efficiency conditioned on the interference vector \mathbf{g}_1 is

$$\eta | \mathbf{g}_1 = 1 - \frac{1}{N} \frac{\mathbf{k}_0^H \mathbf{g}_1 \mathbf{g}_1^H \mathbf{k}_0}{\|\mathbf{k}_0\|^2}. \quad (28)$$

Averaging over the interference vectors \mathbf{g}_1 and accounting for the independence of its components, we have $E [\mathbf{k}_0^H \mathbf{g}_1 \mathbf{g}_1^H \mathbf{k}_0] = \|\mathbf{k}_0\|^2$, hence the asymptotic efficiency of the spatial processor is given by

$$\eta_s = 1 - \frac{1}{N}. \quad (29)$$

It is interesting to note that for a tone interference, the temporal and spatial processors have the same asymptotic efficiency, and both result in the loss of one degree of freedom. Next is investigated the effect of the interference bandwidth on the efficiency of each processor.

INTERFERENCE BANDWIDTH EFFECTS

For the single tone interference, the temporal correlation matrix is given by Equation (14). This matrix has an eigenvalue $\lambda_1 = J' + (|c_0|^2 \mathcal{E} + N_o)$ and $(Q - 1)$ eigenvalues $(|c_0|^2 \mathcal{E} + N_o)$. As the bandwidth of the interference increases, additional eigenvalues raise above the $(|c_0|^2 \mathcal{E} + N_o)$ plateau. A relation between the number of principal eigenvalues r and the bandwidth B is provided by the Landau-Pollak theorem [15]: $r \approx 2B\tau + 1$, where $\tau = (Q - 1)T_d$ is the time duration associated with the PEF structure. The effect of the interference bandwidth on the efficiency of the PEF, can be demonstrated by assuming that \mathbf{R}_t consists of two equal strength and orthogonal vectors, i.e., $\mathbf{R}_t = J' \mathbf{f}_1 \mathbf{f}_1^H + J' \mathbf{f}_2 \mathbf{f}_2^H + (|c_0|^2 \mathcal{E} + \frac{1}{2} N_o) \mathbf{I}_Q$. By successive applications of the matrix inversion lemma, it can be easily shown that as J'/\mathcal{E} , $J'/N_o \rightarrow \infty$,

$$\mathbf{a} = \mathbf{e}_o - \frac{1}{Q} \mathbf{f}_1 - \frac{1}{Q} \mathbf{f}_2. \quad (30)$$

Using steps similar to those leading to Equation (17), the asymptotic efficiency of the PEF for this case is $\eta_t = 1 - \frac{2}{Q}$. This result can be generalized to any number of eigenvalues, i.e., for r principal eigenvalues, the asymptotic efficiency is given by

$$\eta_t = 1 - \frac{r}{Q}. \quad (31)$$

The efficiency decreases to 0 when the interference bandwidth B approaches the spread spectrum bandwidth, ($B = 1/2T_d$). While the PEF performance is governed by the interference

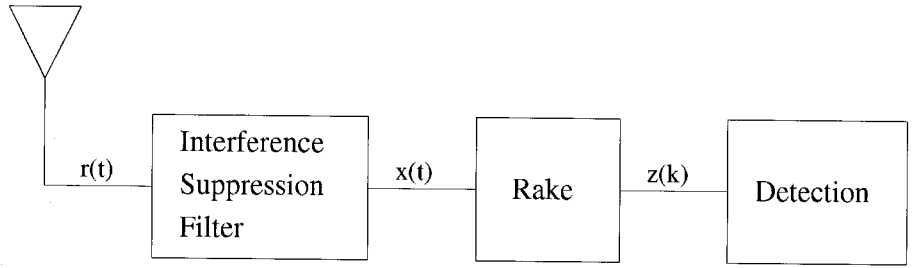


Figure 1. The PEF-Rake receiver.

bandwidth in relation to the spread spectrum signal bandwidth, the spatial processor performance is determined by the ratio of the interference bandwidth to the *carrier frequency*. Thus even a wideband interference is *narrowband spatially*, and the performance is accurately represented by Equation (29). Moreover, not only is the spatial processor robust with respect to the bandwidth, but it also provides diversity paths to mitigate multipath effects.

3. Space-Time Processing

In this section two space-time processing schemes are formulated and their efficiency is compared to a receiver consisting of a interference suppression filter followed by a Rake receiver. We refer to the latter either as PEF-Rake or *time-time*. The PEF-Rake structure has been suggested and analyzed in [5]. Main points from the reference, including necessary adjustments in notation, are provided below.

TIME-TIME PROCESSING

The PEF-Rake structure is shown in Figure 1. Starting with Equation (5), the combined effect of the channel and the interference suppression filter can be expressed as a single linear filtering operation \mathbf{b} such that

$$\mathbf{b}^H \tilde{\mathbf{u}}(t) = \mathbf{a}^H \mathbf{U}^T(t) \mathbf{c}, \quad (32)$$

where $\tilde{\mathbf{u}}(t)$ is the $Q' = (M + Q - 1)$ -dimensional vector $\tilde{\mathbf{u}}^T(t) = [u(t), \dots, u(t - (M + Q - 2)T_d)]$, and \mathbf{b} is the convolution of \mathbf{a} and \mathbf{c} , i.e.

$$b_m = \sum_{k=0}^{M-1} c_k^* a_{m-k}, \quad m = 0, \dots, Q' - 1, \quad (33)$$

where $c_m = 0$ for $m = Q, \dots, Q' - 1$. Then the output of the PEF, Equation (5), can be rewritten in terms of \mathbf{b} :

$$x(t) = \sqrt{\mathcal{E}} \sum_i d(i) \mathbf{b}^H \tilde{\mathbf{u}}(t - iT) + \mathbf{a}^H \mathbf{j}(t) + \mathbf{a}^H \mathbf{v}(t). \quad (34)$$

The Rake receiver consists of delay, demodulation and sum of the Q' signal components. The demodulated input to the Rake can be written:

$$\begin{aligned} y_m(k) &= \langle x(t + mT_d), u(t - kT) \rangle \\ &= d(k) \sqrt{\mathcal{E}} \mathbf{p}_{0,m}^T \mathbf{b} + d(k-1) \sqrt{\mathcal{E}} \mathbf{p}_{-1,m}^T \mathbf{b} + d(k+1) \sqrt{\mathcal{E}} \mathbf{p}_{+1,m}^T \mathbf{b} \\ &\quad + j_{t,m}(k) + v_{t,m}(k) \end{aligned} \quad (35)$$

for $0 \leq m \leq Q' - 1$. The signature waveform cross-correlation vectors are:

$$\mathbf{p}_{\ell,m} = \langle \tilde{\mathbf{u}}(t + mT_d + \ell T), u(t) \rangle, \quad \ell = 0, \pm 1. \quad (36)$$

The interference is given by $j_{t,m}(k) = \mathbf{a}^H \langle \mathbf{j}_t(t + mT_d), u(t) \rangle$, and the noise is defined in a similar manner. Assuming orthogonality of the signature waveforms, $\mathbf{p}_{\ell,m} = \mathbf{e}_m \delta_{\ell 0}$, where \mathbf{e}_m is the unit vector with the m -th element set to 1, and $\delta_{\ell 0}$ is the Kronecker symbol ($\delta_{\ell 0} = 1$, for $\ell = 0$ and it equals zero otherwise). The Q' dimensional vector $\mathbf{y}(k)$ at the input of the Rake receiver can then be written:

$$\mathbf{y}(k) = d(k) \sqrt{\mathcal{E}} \mathbf{b} + \mathbf{j}_{t-t}(k) + \mathbf{v}_{t-t}(k), \quad (37)$$

where $\mathbf{j}_{t-t}^T(k) = [j_{t,0}(k), \dots, j_{t,M-1}(k)]$ and $\mathbf{v}_{t-t}(k)$ is defined in a similar manner. The subscript $t-t$ indicates the cascade of two temporal processes. The Rake receiver is a maximal ratio combiner of the signal vector \mathbf{b} (the channel vector \mathbf{c} modified by the PEF coefficients vector \mathbf{a}). Maximal ratio combining is provided by a weight vector equal to \mathbf{b} . The Rake output can then be written:

$$\begin{aligned} z(k) &= \mathbf{b}^H \mathbf{y}(k) \\ &= \sqrt{\mathcal{E}} d(k) \|\mathbf{b}\|^2 + \mathbf{b}^H \mathbf{j}_{t-t}(k) + \mathbf{b}^H \mathbf{v}_{t-t}(k). \end{aligned} \quad (38)$$

The efficiency of the PEF-Rake structure can be determined based on the following argument: the PEF removes the interference at the cost of an increased noise factor of $\left(1 - \frac{r}{Q}\right)^{-1}$ (see the argument leading to Equation (31)). Although the Rake has Q' taps (the dimension of \mathbf{b}), it provides only an M order diversity (M is the number of independent signal paths in the channel). Hence, the PEF-Rake structure operates as an M diversity receiver with an input noise of $\frac{1}{2} N_o \left(1 - \frac{r}{Q}\right)^{-1}$. To reiterate, the asymptotic efficiency represents the processor's performance with respect to the cancellation of the interference only and it ignores diversity processing. It follows that the asymptotic efficiency of the PEF-Rake is the same as that of the PEF:

$$\eta_{t-t} = \left(1 - \frac{r}{Q}\right). \quad (39)$$

This result is valid for either the case of a single interference with a bandwidth corresponding to r principal eigenvalues, or for r tone interferences. The combined effect of cancellation and diversity is captured in the SNR p.d.f. and error probability calculations in section 4.

CASCADE SPACE-TIME

The general configuration for the cascade space-time receiver is shown in Figure 2. The cascade space-time receiver consists of a antenna array whose outputs are delayed, demodulated, combined spatially and then combined temporally. As explained in section 2, the interference bandwidth has no effect on spatial processing. Since the interference is already canceled at the output of the spatial processors, the asymptotic efficiency of the cascade space-time architecture is the same as that of the spatial processor only. Consider the case of r interferences of arbitrary bandwidth. The space-time architecture has $N \times M$ degrees of freedom. As each of the N spatial processors consumes r degree of freedom in canceling the interference, the

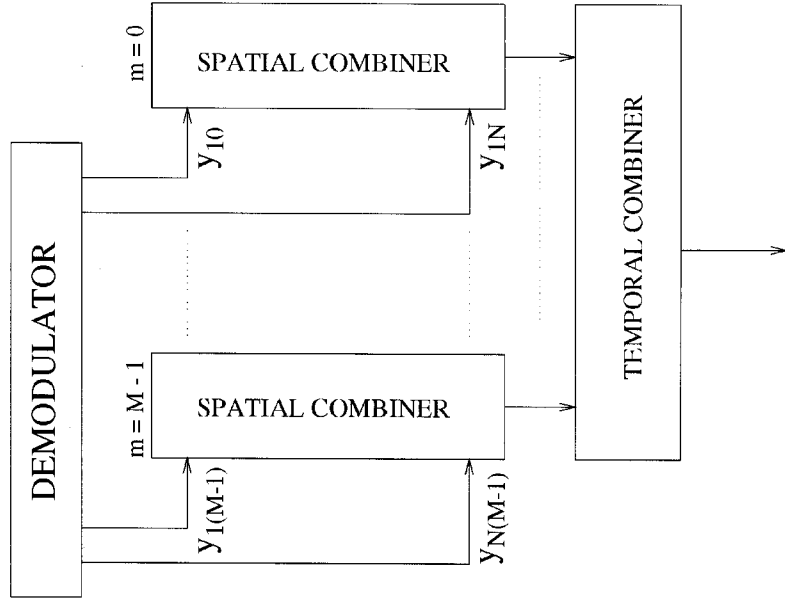


Figure 2. General configuration of the cascade space-time receiver.

total number of degrees of freedom left is $NM - rM$. The asymptotic efficiency of the cascade space-time processor is then

$$\eta_{s-t} = \frac{NM - rM}{NM} = 1 - \frac{r}{N}. \quad (40)$$

The important point to note is that the efficiency of cascade space-time processing is not affected by the interference bandwidth but, obviously, depends on the number of interferences.

JOINT-DOMAIN PROCESSING

The joint domain processor is shown in Figure 3. In the joint-domain receiver architecture, processing is carried out simultaneously in the space and time domains. Let the demodulator outputs $\zeta_{nm}(k)$ in Equation (20) be organized as the elements of an $N \times M$ matrix. Let the symbol $\text{vec}[\zeta_{nm}(k)]$ denote stacking the rows of this matrix to form an NM -dimensional vector. Using this notation, the input to the joint-domain processor is $\mathbf{y}(k) = \text{vec}[\zeta_{nm}(k)]$, which can be written:

$$\mathbf{y}(k) = d(k)\sqrt{\mathcal{E}}\mathbf{q}_0 + d(k-1)\sqrt{\mathcal{E}}\mathbf{q}_{-1} + d(k+1)\sqrt{\mathcal{E}}\mathbf{q}_{+1} + \mathbf{j}_{j-d}(k) + \mathbf{v}_{j-d}(k), \quad (41)$$

where $\mathbf{q}_\ell = \text{vec}[\mathbf{C}[\mathbf{p}_{0,\ell}, \dots, \mathbf{p}_{M-1,\ell}]]$, $\ell = 0, \pm 1$, $\mathbf{p}_{m,\ell}$ is as defined following Equation (20). The joint-domain interference vector is $\mathbf{j}_{j-d}(k) = \text{vec}(j_{nm}(k))$, and the noise is defined in a similar manner. The joint-domain optimal weight vector is given by

$$\mathbf{w} = \mathbf{R}_y^{-1}\mathbf{r}, \quad (42)$$

where $\mathbf{R}_y = E\left[(\mathbf{y}(k) - d(k)\sqrt{\mathcal{E}}\mathbf{q}_0)(\mathbf{y}(k) - d(k)\sqrt{\mathcal{E}}\mathbf{q}_0)^H\right]$ and $\mathbf{r} = E[d(k)\mathbf{y}(k)] = \sqrt{\mathcal{E}}\mathbf{q}_0$.

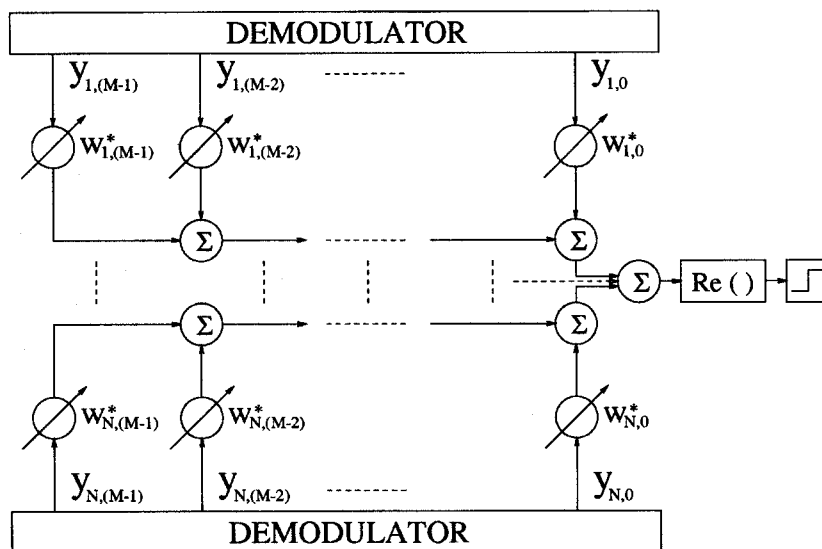


Figure 3. General configuration of the joint-domain receiver.

The effect of the interference bandwidth on joint-domain processing can be assessed from the interference vector $\mathbf{j}_{j-d}(k)$ structure. For the case of a single tone, the interference can be expressed $\mathbf{j}_{j-d}(k) = \sqrt{J} \mathbf{f}_1 \otimes \mathbf{g}_1$, where \mathbf{f}_1 is an M -dimensional temporal vector, \mathbf{g}_1 is an N -dimensional spatial vector, and \otimes denotes the Kronecker product (i.e., the vector $\mathbf{f}_1 \otimes \mathbf{g}_1$ has NM elements, the j th element is given by $(\mathbf{f}_1)_{1+[j/N]} (\mathbf{g}_1)_{j \bmod N}$). A multiple tone interference will be represented by multiple vectors in the joint-domain, since $(\mathbf{f}_1 + \mathbf{f}_2) \otimes \mathbf{g}_1 = \mathbf{f}_1 \otimes \mathbf{g}_1 + \mathbf{f}_2 \otimes \mathbf{g}_1$. There are NM degrees of freedom available to the joint-domain processing. A narrowband interference represented by $r \leq M$ principal eigenvalues will capture r degrees of freedom of the joint-domain. The number of degrees of freedom left for diversity processing is therefore $NM - r$, and the asymptotic efficiency of the joint-domain processor is

$$\eta_{j-d} = 1 - \frac{r}{NM}. \quad (43)$$

This expression applies equally for a single interference with r principal eigenvalues or r tone interferences. Comparison of expressions (39), (40), and (43) shows that the asymptotic efficiencies of the three processors considered are related as

$$\eta_{j-d} \geq \eta_{s-t} \geq \eta_{t-t}. \quad (44)$$

This relation applies for either single or multiple interferences. Thus joint-domain is superior to cascade space-time, and cascade space-time in turn outperforms the PEF-Rake combination.

4. Error Probability Computations

In the previous section, expressions were developed for the asymptotic efficiency of several processing schemes. This resulted in simple expressions that capture the essence of the performance of each method. In this section, we undertake a detailed performance analysis. Due to the fading environment, the SNR at the output of each processor is modeled as a random variable. The objective here is to characterize the p.d.f. of the SNR at the output of each processor, and use it to evaluate the average probability of error.

TIME-TIME PROCESSING

In the case of a narrowband interference whose power is spread over several eigenvalues, the asymptotic efficiency of the PEF-Rake receiver is given by Equation (39). Since in the absence of the interference, the SNR of the receiver is $2\mu = \mathcal{E}/\frac{1}{2}N_o \sum_{m=0}^{M-1} |c_m|^2$, it follows that the effective SNR at the output of the PEF-Rake receiver is,

$$\mu = \frac{\mathcal{E}}{N_o} \left(1 - \frac{r}{Q}\right) \sum_{m=0}^{M-1} |c_m|^2. \quad (45)$$

Since the channel coefficients are assumed $c_m \sim \text{CN}[0, 1]$, $|c_m|$ is Rayleigh-distributed, $|c_m|^2$ has a χ_2^2 distribution (chi-square with 2 degrees of freedom), and $\frac{\mathcal{E}}{N_o} \left(1 - \frac{r}{Q}\right) |c_m|^2$ has an exponential distribution with parameter $\left(\frac{\mathcal{E}}{N_o} \left(1 - \frac{r}{Q}\right)\right)^{-1}$ (this distribution is denoted $\exp\left[\left(\frac{\mathcal{E}}{N_o} \left(1 - \frac{r}{Q}\right)\right)^{-1}\right]$). The average probability of error is simply [16]:

$$P_e = \int_0^\infty Q(\sqrt{2\mu}) f(\mu) d\mu, \quad (46)$$

where $Q(\cdot)$ is the gaussian tail function. The SNR μ is the sum of M exponential $\exp\left[\left(\frac{\mathcal{E}}{N_o} \left(1 - \frac{r}{Q}\right)\right)^{-1}\right]$ variables, hence it has a $\Gamma(M, \gamma^{-1})$ gamma distribution² with parameters M and γ^{-1} , $\Gamma(M, \gamma^{-1}) = f(\mu) = \Gamma^{-1}(M) \gamma^{-M} \mu^{M-1} e^{-\mu/\gamma}$, where $\Gamma(M) = (M-1)!$, $\gamma = E[\mu] = \left(1 - \frac{r}{Q}\right) \gamma_o$, and $\gamma_o = \mathcal{E}N_o^{-1}$. An upper bound on the error probability can be obtained by noting that $Q(\sqrt{2\mu}) = \frac{1}{2} \text{erfc} \sqrt{\mu} < \frac{e^{-\mu}}{2\sqrt{\pi}} < e^{-\mu}$. While there are tighter bounds available, this bound is simple and affords insight in the final results. Using this relation in (46) we obtain

$$P_e < \Gamma^{-1}(M) \gamma^{-M} \int_0^\infty \mu^{M-1} e^{-(1+\gamma^{-1})\mu} d\mu. \quad (47)$$

If we identify $s = 1 + 1/\gamma$, the expression above is a Laplace transform. Using the Laplace pair $\Gamma^{-1}(M) \mu^{M-1} \leftrightarrow s^{-M} = (1 + 1/\gamma)^{-M}$, it follows that

$$\begin{aligned} P_{e,t-t} &< (1 + \gamma)^{-M} \\ &= \left(1 - \left(1 - \frac{r}{Q}\right) \gamma_o\right)^{-M} \\ &\approx \left(1 - \frac{r}{Q}\right)^{-M} \gamma_o^{-M} \end{aligned} \quad (48)$$

for $\gamma \gg 1$. In the absence of interference, the upper bound is $P_{e,t-t} < \gamma_o^{-M}$. Comparison of the error probability expressions with and without interference clearly demonstrates the performance loss due to the presence of the interference.

² In this paper we distinguish between a χ_2^2 variable (the magnitude squared of CN [0, 1]) and an $\exp[\lambda]$ variable (the magnitude squared of CN [0, λ^{-1}]). Occasionally, authors do not make this discrimination, and consequently do not discern between the sum of M χ_2^2 variables, which is χ_{2M}^2 , and the sum of M $\exp[\lambda]$ variables, which is $\Gamma(M, \lambda)$.

SPACE-TIME PROCESSING

In this section we develop expressions for the error probability with space and space-time processing in a Rayleigh channel and in the presence of non-fading narrowband interferences. We start with a stand-alone spatial combiner and proceed to the cascade space-time and joint-domain combiners.

Spatial Combiner

For the spatial combiner defined by Equation (23), the effective SNR at the array output is given by

$$\mu = \mathcal{E} \mathbf{k}_0^H \mathbf{R}_{\zeta_0}^{-1} \mathbf{k}_0. \quad (49)$$

Since the channel vector \mathbf{k}_0 is random, the SNR μ is a random variable. The p.d.f. of μ for the case of a single interference was characterized by Bogachev and Kiselev, [13]. We apply their approach, generalize their results to r interferences, and use the p.d.f. to develop a closed-form expression for an upper bound on the error probability. An upper bound for the error probability for multiple interferences when $N_o \rightarrow 0$ was obtained by Winters et. al., [8] using mean square error considerations. Our approach is different, in that it builds on the p.d.f. of the SNR, and our results are more general in the sense that the dependency on the interference power is explicit.

The eigen-decomposition of the interference+noise matrix $\mathbf{R}_{\zeta_0}^{-1}$ can be written

$$\mathbf{R}_{\zeta_0}^{-1} = \sum_{n=1}^N (\lambda_n + N_o)^{-1} \mathbf{q}_n \mathbf{q}_n^H, \quad (50)$$

where λ_n are the interference eigenvalues and N_o is the noise power. When there are $r \leq N$ interferences present (tone or narrowband), $\mathbf{R}_{\zeta_0}^{-1} = \sum_{n=1}^r (\lambda_n + N_o)^{-1} \mathbf{q}_n \mathbf{q}_n^H + N_o^{-1} \sum_{n=r+1}^N \mathbf{q}_n \mathbf{q}_n^H$. Consequently, we can write

$$\mathbf{k}_0^H \mathbf{R}_{\zeta_0}^{-1} \mathbf{k}_0 = \sum_{n=1}^r (\lambda_n + N_o)^{-1} \left| \mathbf{k}_0^H \mathbf{q}_n \right|^2 + N_o^{-1} \sum_{n=r+1}^N \left| \mathbf{k}_0^H \mathbf{q}_n \right|^2. \quad (51)$$

The eigenvectors \mathbf{q}_n provide a unitary transformation which retains the properties of the components of \mathbf{k}_0 . Assuming that $\mathbf{k}_0 \sim \text{CN}[\mathbf{0}, \mathbf{I}_N]$, the quantities $(\lambda_n + N_o)^{-1} \left| \mathbf{k}_0^H \mathbf{q}_n \right|^2$ have a distribution $\exp[-(\lambda_n + N_o)]$. The random variable μ is obtained as the sum of N (not necessarily equal mean) independent exponential random variables. The characteristic function (c.f.) of each exponential variable is $\Psi_{\gamma_n}(j\nu) = 1/(1 - j\nu\gamma_n)$, where $\gamma_n = \mathcal{E}(\lambda_n + N_o)^{-1} E \left[\left| \mathbf{k}_0^H \mathbf{q}_n \right|^2 \right] = \mathcal{E}(\lambda_n + N_o)^{-1}$, for $n = 1, \dots, r$, and $\gamma_n = \mathcal{E}N_o^{-1} \equiv \gamma_o$ for $n = r + 1, \dots, N$. The c.f. of μ is given by:

$$\Psi_{\mu}(j\nu) = \left(\prod_{k=1}^r \frac{1}{(1 - j\nu\gamma_k)} \right) \frac{1}{(1 - j\nu\gamma_o)^{N-r}}. \quad (52)$$

We first consider the case when the r sources are equal power and are represented by mutually orthogonal vectors, such that $\gamma_k = \gamma_i$ for $k = 1, \dots, r$. Orthogonality between the sources represents a worst case from the performance point of view. In this case, the c.f. becomes

$$\Psi_{\mu}(j\nu) = \frac{1}{(1 - j\nu\gamma_i)^r (1 - j\nu\gamma_o)^{N-r}}. \quad (53)$$

The p.d.f. of μ is computed in appendix A. In the appendix it is also shown that for large μ , the p.d.f. can be approximated by the relation

$$f(\mu) = \Gamma^{-1}(N-r) \gamma_o^{-(N-r)} \mu^{N-r-1} e^{-\mu/\gamma_o}. \quad (54)$$

In the absence of interferences ($r = 0$), this relation reverts to a $\Gamma(N, \gamma_o^{-1})$ p.d.f., as it should. The significance of Equation (54) is that it demonstrates the loss of r degrees of freedom due to the presence of narrowband interference. An expression of the p.d.f. $f(\mu)$ explicitly dependent on the interference power is provided in the appendix. The general case, when the interference eigenvalues are not equal, is treated in appendix B. The error probability for the optimal spatial combiner in a flat Rayleigh channel with multiple interferers is computed in appendix C. In the appendix, expressions are derived for both the general case, as well as the special case of orthogonal and equal power interferers. For the latter case, it is shown that an upper bound on the error probability is given by

$$P_e < (1 + \gamma_i)^{-r} (1 + \gamma_o)^{-(N-r)}. \quad (55)$$

A few special cases are noteworthy:

1. When there are no interferences $\gamma_i = \gamma_o$, and $P_e < (1 + \gamma_o)^{-N} \approx \gamma_o^{-N}$. This is the well known relation of the error probability in a fading channel with diversity.
2. When the interferences power is very large $\gamma_i \rightarrow 0$, and $P_e < (1 + \gamma_o)^{-(N-r)} \approx \gamma_o^{-(N-r)}$. This relation once more demonstrates the loss of r diversity degrees of freedom due to the presence of the r interferences.

Using the results of Appendices B and C, it is straightforward to show that for non-equal interference eigenvalues the error probability bound is given by,

$$P_e < \sum_{k=1}^r \pi_k (1 + \gamma_k)^{-1} (1 + \gamma_o)^{-(N-r)}, \quad (56)$$

where $\pi_k = \prod_{j=1, j \neq k}^r \frac{\gamma_k}{\gamma_k - \gamma_j}$.

Cascade Space-Time

As explained in section 3, the cascade space-time scheme consists of weighting and summing the outputs of M spatial combiners. The output SNR for this scheme is then, $\mu_{s-t} = \sum_{m=0}^{M-1} \mu_m$, where μ_m is the SNR associated with each spatial combiner. All μ_m have the same p.d.f., given by Equation (54). Since the μ_m 's are independent, the c.f. of μ_{s-t} is given by

$$\Psi_{\mu_{s-t}}(j\nu) = [\Psi_{\mu_m}(j\nu)]^M. \quad (57)$$

Retracing the steps that lead to the result in expression (54), we obtain for a single interference ($r = 1$)

$$f(\mu_{s-t}) = \Gamma^{-1}((N-1)M) \gamma_1^{-1} \gamma_o^{-(N-1)M} \mu^{(N-1)M-1} e^{-\mu_{s-t}/\gamma_1} {}_1F_1 \left[N-1, N; \left(\gamma_1^{-1} - \gamma_o^{-1} \right) \mu_{s-t} \right], \quad (58)$$

where ${}_1F_1$ is the confluent hypergeometric function defined in Appendix A. For large interference $J'/\mathcal{E} \rightarrow \infty$ (i.e., $\gamma_1 = \mathcal{E}(\lambda_n + N_o)^{-1} = \mathcal{E}(J' + N_o)^{-1} \rightarrow 0$) simplifies to:

$$f(\mu_{s-t}) = \Gamma^{-1}((N-1)M) \gamma_o^{-(N-1)M} \mu_{s-t}^{(N-1)M-1} e^{-\mu_{s-t}/\gamma_o}. \quad (59)$$

From Equation (59) and from appendix C, it can be shown that the bound on the error probability is

$$P_{e,s-t} < (1 + \gamma_1)^{-1} (1 + \gamma_o)^{-(N-1)M}. \quad (60)$$

This relation demonstrate the loss of M degrees of freedom incurred by the cascade space-time processing due to the interference cancellation. This conclusion supports the result reached in Equation (40) (note that the loss of M DOF out of NM corresponds to an efficiency of $1 - 1/N$). The expression above can be generalized to the case of r interferences:

$$P_{e,s-t} < \sum_{k=1}^r \pi_k (1 + \gamma_k)^{-1} (1 + \gamma_o)^{-(N-r)M}. \quad (61)$$

Joint-Domain

From the presentation in section 3, in the case of a single narrowband interference, the interference+noise covariance matrix in joint space-time domain is characterized by $r \leq M$ principal eigenvalues. The number of principal eigenvalues is determined by the interference bandwidth. In general, the interference eigenvalues do not have equal magnitude. The c.f. of the SNR at the output of the joint-domain processor is given by

$$\Psi_{\mu_{j-d}}(j\nu) = \left(\prod_{k=1}^r \frac{1}{(1 - j\nu\gamma_k)} \right) \frac{1}{(1 - j\nu\gamma_o)^{NM-r}}. \quad (62)$$

Using an approach similar to the one in appendix B, and substituting $NM \rightarrow N$ in Equation (76), we find that the p.d.f. of the SNR at the output of a joint-domain combiner in a Rayleigh fading channel in the presence of a single interference with r principal eigenvalues is given by

$$f(\mu_{j-d}) = \Gamma^{-1}(NM - r + 1) \sum_{k=1}^r \pi_k \gamma_k^{-1} \gamma_o^{-(NM-r)} \mu_{j-d}^{NM-r} e^{-\mu_{j-d}/\gamma_k} {}_1F_1 \left[NM - r, NM - r + 1; \left(\gamma_k^{-1} - \gamma_o^{-1} \right) \mu_{j-d} \right].$$

Using results from appendices B and C, it can be shown that the upper bound on the error probability for the joint-domain case is given by,

$$P_{e,j-d} < \sum_{k=1}^r \pi_k (1 + \gamma_k)^{-1} (1 + \gamma_o)^{-(NM-r)}. \quad (63)$$

To appreciate the significance of these results, it is useful to compare the error probabilities in expressions (48), (61), and (63). Starting with Equation (48), note that $\gamma = \left(1 - \frac{r}{Q}\right) \gamma_o \leq \gamma_o$. Hence, for $N > 1, M > 1$,

$$P_{e,t-t} \approx (1 + \gamma)^{-M} \geq (1 + \gamma_o)^{-M} \geq (1 + \gamma_1)^{-1} (1 + \gamma_o)^{-(N-1)M} \approx P_{e,s-t}. \quad (64)$$

To compare $P_{e,s-t}$ and $P_{e,j-d}$, note that in Equation (63), $\sum_{k=1}^r \pi_k (1 + \gamma_k)^{-1} = \prod_{k=1}^r (1 + \gamma_k)^{-1} \leq (1 + \gamma_1)^{-r}$, where $\gamma_1 = \max_k \gamma_k$. Consequently, for $r \leq M$,

$$\begin{aligned} P_{e,j-d} &\approx \sum_{k=1}^r \pi_k (1 + \gamma_k)^{-1} (1 + \gamma_o)^{-(NM-r)} \leq (1 + \gamma_1)^{-1} (1 + \gamma_o)^{-(N-1)M} \\ &\approx P_{e,s-t}. \end{aligned} \quad (65)$$

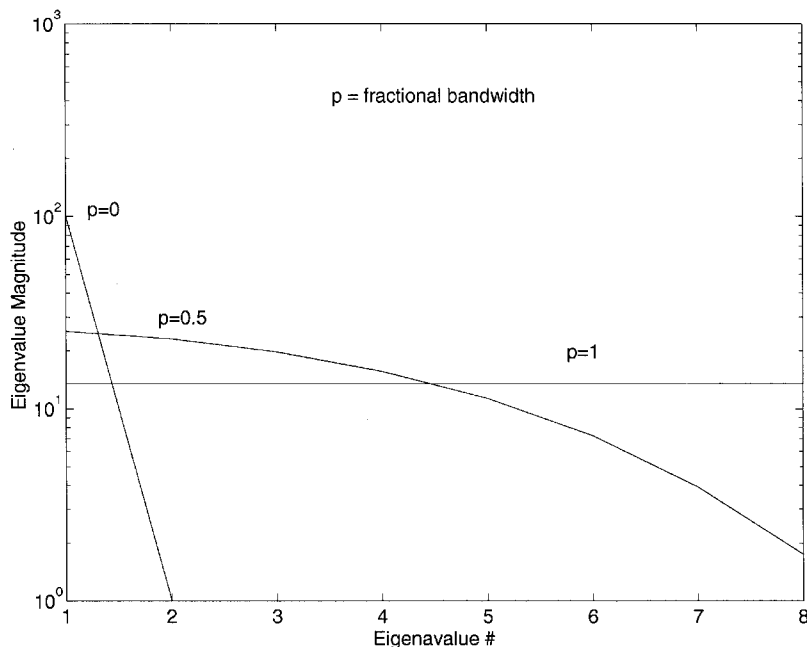


Figure 4. Dependency of eigenvalues of the temporal correlation matrix on bandwidth.

It follows that the relation between the performances of the various methods is:

$$P_{e,j-d} \leq P_{e,s-t} \leq P_{e,j-d}. \quad (66)$$

5. Numerical Results

The numerical results section consists of two parts. In the first part, numerical evaluations of the asymptotic efficiency are provided. The second part consists of simulation results.

The effect of the interference bandwidth on the temporal correlation matrix is shown in Figure 4. Assuming a pulse-train waveform with symbol interval T_j , the autocorrelation of the interference samples is given by

$$r_j(mT_c) = J'(1 - |m|p) e^{-j\pi qm} \quad (67)$$

where $p = T_c/T_j$ is the interference fractional bandwidth, and $q = \Omega T_c/\pi$ is the normalized offset frequency. Note that both p and q are unitless, and that $0 \leq p \leq 1$, $|q| \leq 1$. In Figure 4 the eigenvalues of $\mathbf{R}_j + \mathbf{I}_Q$, where \mathbf{R}_j is the interference correlation matrix, and \mathbf{I}_Q is the Q -dimensional unit matrix, are plotted for $Q = 8$, and several values of the bandwidth p . It is clear from the figure that the number of principal eigenvalues increases with p . The effect of the number of principal eigenvalues on the efficiency of the PEF can be seen from Figure 5. For fractional bandwidth = 0 (tone interference), and large INR, the efficiency $\eta_t = 1 - 1/8 = 7/8$. The efficiency decreases rapidly as the bandwidth increases. Comparison of the efficiencies of the PEF-Rake, cascade space-time and joint-domain processors, is shown in Figure 6. Results are presented for $Q = M = N = 4$ and INR = 20 dB (after spread spectrum processing). Shown are averages of 500 runs over random values of the channels, the parameter q , and the interference phases at the array elements ψ_n . The conditional efficiency for each run and each

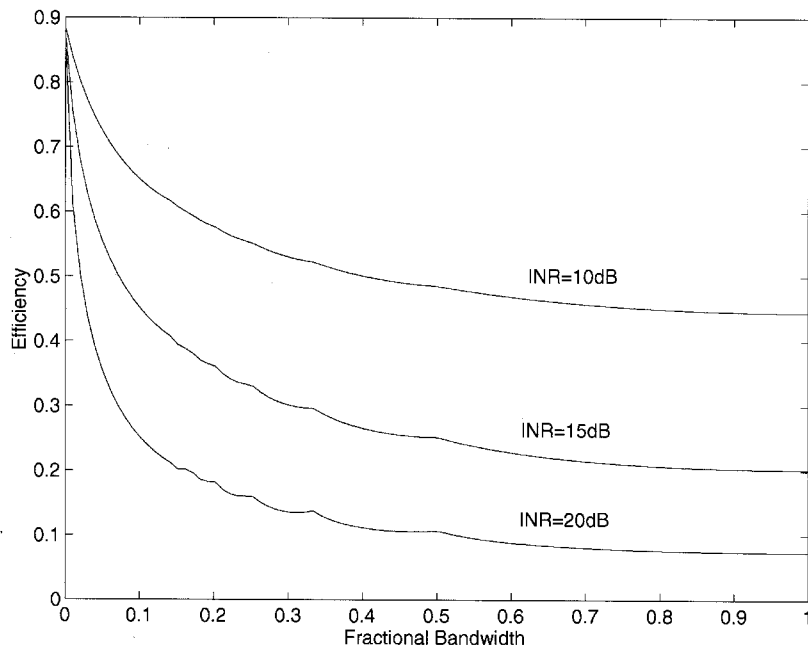


Figure 5. Efficiency of temporal interference suppression.

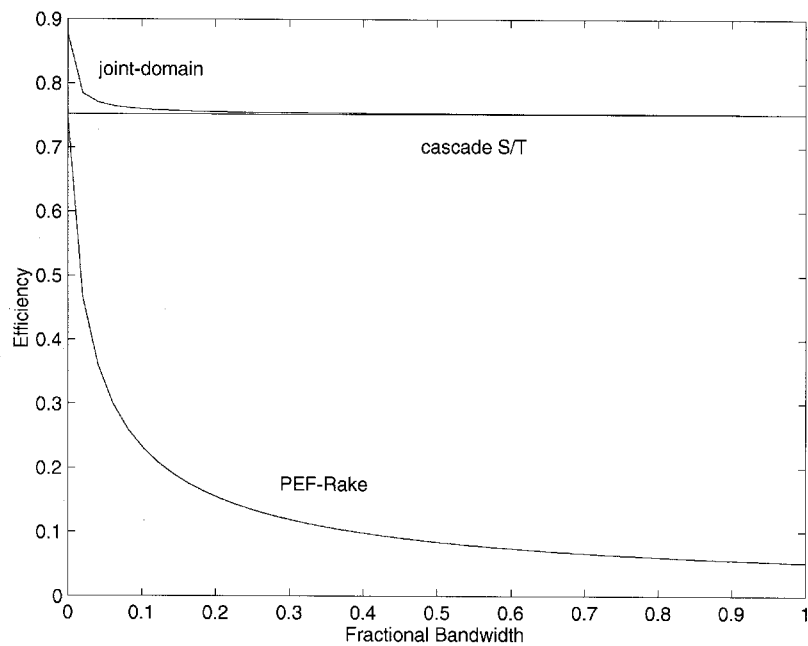


Figure 6. Efficiency of PEF-Rake, cascade, and joint-domain processors.

processor was computed using the definition, and then the results were averaged. The figure clearly demonstrates relation (44).

The simulation model assumed an $M = 4$ four-tap channel model and a two element antenna array ($N = 2$). The curves were generated averaging 200 Monte Carlo runs at each

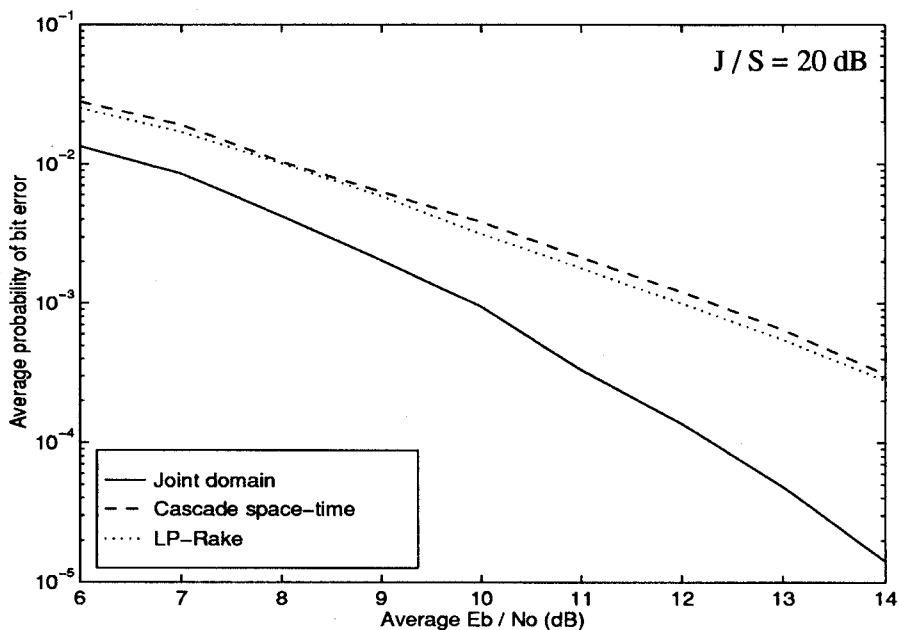


Figure 7. Bit error rate for the case of tone interference.

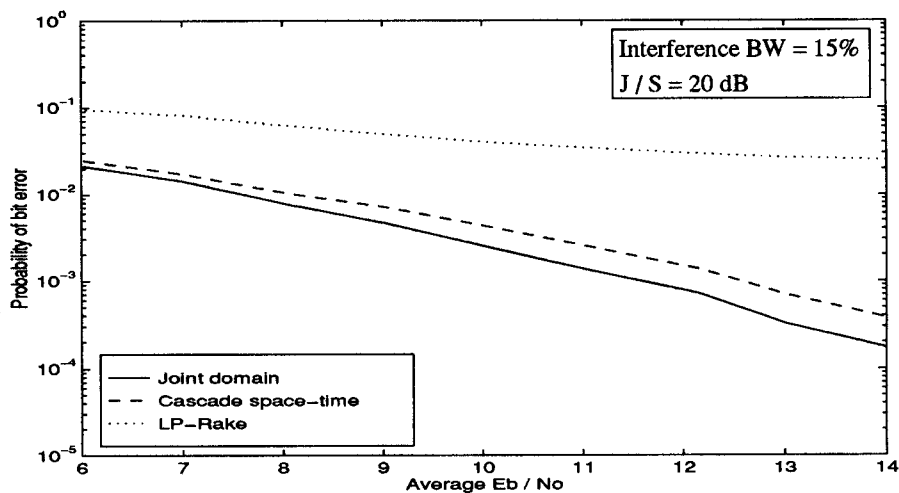


Figure 8. Bit error rate for the case of bpsk interference.

E_b/N_0 point. For the space-time structures, the weight vectors were computed based on block estimates of the various correlation matrices. The number of samples utilized in the estimates was 51. The spreading sequence had a length of 31. The coefficients of the PEF and the Rake were computed using an RLS algorithm as described in [5]. The number of coefficients of the PEF was $Q = 5$. The interference frequency/phase across the array, were varied randomly at each run. The performance of the PEF-Rake, cascade space-time, and joint-domain receivers is compared in each of the figures below. Figure 7 shows the bit error rate for the case of a tone interference. The cascade and the PEF-Rake receivers present almost the same performance. Indeed, both are diversity receivers of order 4. The slight advantage in the

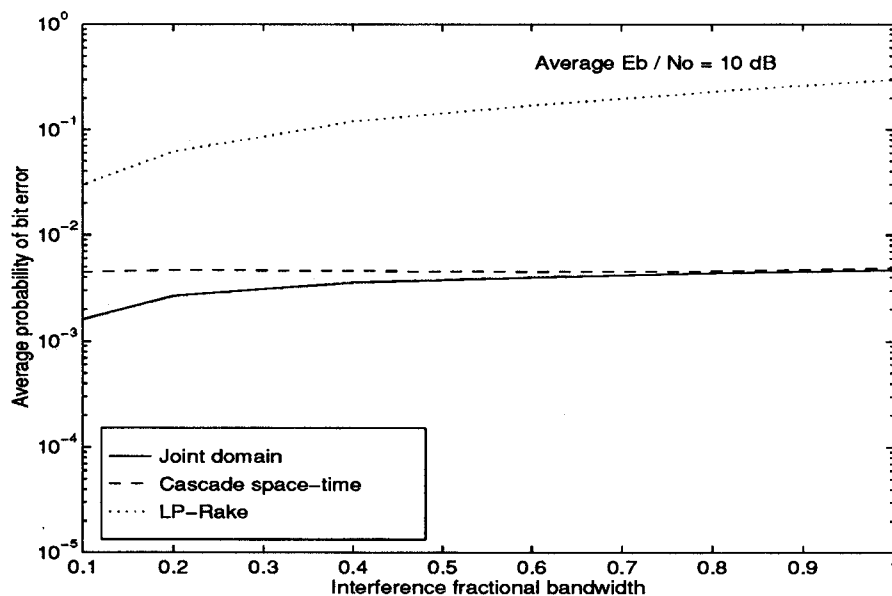


Figure 9. Effect of interference bandwidth.

cascade space-time configuration over the time-time configuration is due to the $(1 - 1/Q)^{-1}$ increase in the noise with the latter, as explained in section 3. The joint-domain performance is characterized by an order $(NM - 1 = 7)$ diversity hence it provides better performance. In Figure 8, the interference bandwidth is increased to 15%. The PEF-Rake performance degrades considerably and the cascade receiver is unaffected, as expected from the analysis. The joint-domain receiver loses additional degrees of freedom compared to the tone case, hence its performance also degrades. In Figure 9 the probability of error is plotted vs. the ratio of the interference bandwidth to the spread spectrum bandwidth. It is interesting to note that, as predicted by expression (40), the cascade receiver's performance is unaffected by the bandwidth. From Equations (40) and (43), the performance of the cascade receiver is a lower bound on the performance of the joint-domain receiver. Indeed, Figure 9 shows that for an interference with the same bandwidth as the spread spectrum signal, both space-time architectures have the same probability of error.

6. Conclusions

In this paper we investigated the application of space-time processing to narrowband interference suppression in CDMA communications. Unlike interference suppression by a whitening filter, spatial processing was shown to be insensitive to the interference bandwidth. The performance of several receiver structures was analyzed through their asymptotic efficiency and evaluation of the error probability. The joint-domain receiver was shown to outperform the cascade space-time receiver, and the performance of the latter surpassed the PEF-Rake configuration. Numerical results corroborated those conclusions.

Appendix

A. P.D.F. of Spatial Combiner SNR, Equal Eigenvalues

In this appendix, relation (54) is derived for the p.d.f. of μ . The SNR μ is defined in Equation (49). The objective is to compute the Fourier transform of the c.f. in Equation (53). Identifying $s = -j\nu$, $\rho = \gamma_i^{-1}$, $\sigma = \gamma_o^{-1}$, the following Laplace transform pair is applicable [17, page 410]:

$$\frac{1}{(s + \rho)^{\alpha+\beta} (s + \sigma)^{\alpha-\beta}} \leftrightarrow \Gamma^{-1} (2\alpha) (\rho - \sigma)^{-\alpha} \mu^{\alpha-1} e^{-(\rho+\sigma)\mu/2} M_{\beta, \alpha-\frac{1}{2}} [(\rho - \sigma)\mu], \quad (68)$$

where

$$M(\beta, \xi, z) = z^{\xi+\frac{1}{2}} e^{-z/2} {}_1F_1\left(\xi - \beta + \frac{1}{2}, 2\xi + 1; z\right), \quad (69)$$

and ${}_1F_1$ is the confluent hypergeometric function defined as

$${}_1F_1(a, b; z) = \frac{\Gamma(b)}{\Gamma(b-a)\Gamma(a)} \int_0^1 e^{zt} t^{a-1} (1-t)^{b-a-1} dt. \quad (70)$$

Now identify

$$\begin{aligned} \alpha + \beta &= r \\ \alpha - \beta &= N - r \end{aligned}$$

These relations yield $\alpha = N/2$ and $\beta = r - N/2$. Applying the transform (68) to Equation (53), and utilizing Equation (69), yields after some manipulations

$$f(\mu) = \Gamma^{-1}(N) \rho^r \sigma^{(N-r)} \mu^{N-1} e^{-\rho\mu} {}_1F_1[N - r, N; (\rho - \sigma)\mu]. \quad (71)$$

This relation represents the p.d.f. of the output SNR of a spatial combiner in a flat Rayleigh channel for r equal power and orthogonal interferences. Note the explicit dependency of Equation (71) on the interferences' power. Special cases of relation (71):

1. No interference, $\rho = \sigma = \gamma_o^{-1}$. In this case ${}_1F_1$ simplifies to

$$\begin{aligned} {}_1F_1(N - r, N; 0) &= \frac{\Gamma(N)}{\Gamma(r)\Gamma(N-r)} \int_0^1 t^{N-r-1} (1-t)^{r-1} dt \\ &= \frac{\Gamma(N)}{\Gamma(r)\Gamma(N-r)} B(N - r, r) \\ &= 1, \end{aligned} \quad (72)$$

where $B(v, w) = \int_0^1 t^{v-1} (1-t)^{w-1} dt$ is the beta function, and we used relation 6.2.2 in [18]. Applying this result to Equation (71) results in the p.d.f. of $\Gamma(N, \gamma_o^{-1})$, i.e., an N -diversity receiver, as expected.

2. Large interference power $\gamma_i \ll \gamma_o$, or $\rho \gg \sigma$. Using the asymptotic expansion of ${}_1F_1$ [19, relation (10.45)], we obtain

$${}_1F_1[N - r, N; (\rho - \sigma)\mu] \approx \frac{\Gamma(N)}{\Gamma(N-r)} \frac{e^{(\rho-\sigma)\mu}}{[(\rho - \sigma)\mu]^r}. \quad (73)$$

When the last relation is substituted in (71), we obtain

$$f(\mu) = \Gamma^{-1}(N-r) \sigma^{(N-r)} \mu^{N-r-1} e^{-\mu\sigma} \quad (74)$$

which, upon substituting $\gamma_o = \sigma^{-1}$, is the desired result of Equation (54).

B. P.D.F. of Spatial Combiner SNR, Unequal Eigenvalues

In this appendix, the goal is to develop an expression for the p.d.f. of the SNR μ when the interference eigenvalues are not equal. Starting with the c.f. in Equation (52), we apply the partial fraction expansion

$$\prod_{k=1}^r \frac{1}{(\rho_k - j\nu)} = \sum_{k=1}^r \frac{\pi_k}{\rho_k - j\nu}, \quad (75)$$

where $\rho_k = \gamma_k^{-1}$ and $\pi_k = \prod_{j=1, j \neq k}^r \frac{\rho_j}{\rho_j - \rho_k}$. Substituting this result back into Equation (52), exchanging $N - r + 1 \rightarrow N$, and using the transform (68), it can be shown that

$$f(\mu) = \Gamma^{-1}(N - r + 1) \sum_{k=1}^r \pi_k \rho_k \sigma^{(N-r)} \mu^{N-r} e^{-\rho_k \mu} {}_1F_1 [N - r, N - r + 1; (\rho_k - \sigma) \mu]. \quad (76)$$

This expression represents the general p.d.f. of the output SNR of an optimal spatial combiner in a flat Rayleigh channel with r interferences.

C. Error Probability, Equal Eigenvalues

In this appendix, expressions are derived for the error probability of the optimal spatial combiner in a Rayleigh channel with multiple interferers, for the general case, as well as the special case of orthogonal and equal power interferers. We start with the derivation of expression (55). It is necessary to evaluate $P_e = \int_0^\infty Q(\sqrt{2\mu}) f(\mu) d\mu$, where $f(\mu)$ is given by Equation (71). Using the bound $Q(\sqrt{2\mu}) < e^{-\mu}$, we have

$$P_e < \Gamma^{-1}(N) \rho^r \sigma^{(N-r)} \int_0^\infty \mu^{N-1} e^{-(1+\rho)\mu} {}_1F_1 [N - r, N; (\rho - \sigma) \mu] d\mu. \quad (77)$$

Identifying $s = 1 + \rho$, this is a Laplace transform, for which the solution is found in [20, relation 5.2.4.6, page 96]:

$$\int_0^\infty e^{-s\mu} \mu^{N-1} {}_1F_1 [N - r, N; (\rho - \sigma) \mu] d\mu = \frac{\Gamma(N)}{(1 + \rho)^{N-r}} \left(1 - \frac{\rho - \sigma}{1 + \rho}\right)^{-(N-r)}. \quad (78)$$

Substituting Equation (78) into Equation (77), we obtain

$$P_e < \left(\frac{\rho}{1 + \rho}\right)^r \left(\frac{\sigma}{1 + \sigma}\right)^{N-r}, \quad (79)$$

from which relation (55) follows.

An exact expression for the error probability, albeit not quite as useful as the bound found above, can be obtained in terms of the generalized hypergeometric function. The gaussian tail function can be expressed in terms of ${}_1F_1$ function as follows [18, relation 7.1.21]:

$$\begin{aligned} Q(\sqrt{2\mu}) &= \frac{1}{2} [1 - \operatorname{erf}(\sqrt{\mu})] \\ &= \frac{1}{2} \left[1 - \frac{2\sqrt{\mu}}{\sqrt{\pi}} {}_1F_1 \left(\frac{1}{2}, \frac{3}{2}; -\mu\right)\right]. \end{aligned} \quad (80)$$

To evaluate the error probability $P_e = \int_0^\infty Q(\sqrt{2\mu}) f(\mu) d\mu$, where $f(\mu)$ is given by Equation (71), it is necessary to evaluate the expression

$$I = \int_0^\infty e^{-\rho\mu} \mu^{(N+\frac{1}{2})-1} {}_1F_1\left(\frac{1}{2}, \frac{3}{2}; -\mu\right) {}_1F_1[N-r, N; (\rho-\sigma)\mu] d\mu. \quad (81)$$

Using [20, relation 5.2.4.22, page 98], this is found to be

$$I = \Gamma\left(N + \frac{1}{2}\right) \rho^{-(N+\frac{1}{2})} F_2\left(N + \frac{1}{2}, \frac{1}{2}; N-r; \frac{3}{2}, N; -\frac{1}{\rho}, \frac{\rho-\sigma}{\rho}\right), \quad (82)$$

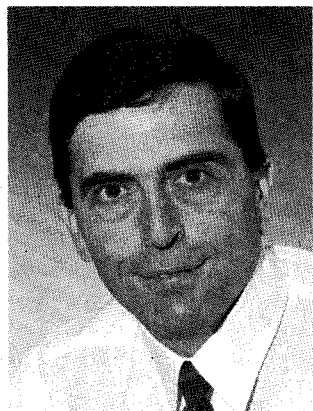
where F_2 is the generalized hypergeometric function. Unfortunately, no closed form is available for F_2 and it is necessary to use its series expansion [20, relation 1.3.2, page 23]. Using Equations (71), (80) and (82), we obtain the following expression for the error probability:

$$P_e = \frac{1}{2} - \frac{\Gamma\left(N + \frac{1}{2}\right)}{\sqrt{\pi\rho}\Gamma(N)} \sigma^{(N-r)} F_2\left(N + \frac{1}{2}, \frac{1}{2}; N-r; \frac{3}{2}, N; -\frac{1}{\rho}, \frac{\rho-\sigma}{\rho}\right). \quad (83)$$

References

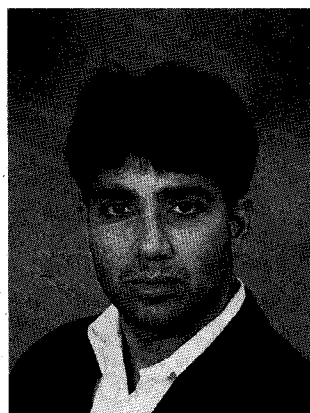
1. L.B. Milstein et al., "On the Feasibility of a CDMA Overlay for Personal Communications Networks", *IEEE Journal on Selected Areas in Communications*, Vol. 10, No. 4, pp. 655-668, 1992.
2. J. Wang and L.B. Milstein, "CDMA Overlay Situations for Microcellular Mobile Communications", *IEEE Trans. Commun.*, Vol. 43, No. 2/3/4, pp. 603-614, 1995.
3. J.W. Ketchum and J.G. Proakis, "Adaptive Algorithms for Estimating and Suppressing Narrow-Band Interference in PN Spread-Spectrum Systems", *IEEE Trans. Commun.*, Vol. 30, pp. 913-923, 1982.
4. L.B. Milstein, "Interference Rejection Techniques in Spread Spectrum Communications", *Proceedings of the IEEE*, Vol. 76, pp. 657-671, 1988.
5. R.A. Iltis, "A GLRT-Based Spread-Spectrum Receiver for Joint Channel Estimation and Interference Suppression", *IEEE Trans. Commun.*, Vol. COM-37, pp. 277-288, 1989.
6. R. Vijayan and H.V. Poor, "Nonlinear Techniques for Interference Suppression in Spread-Spectrum Systems", *IEEE Trans. Commun.*, Vol. 38, pp. 1060-1065, 1990.
7. L. Rusch and H.V. Poor, "Multiuser Detection Techniques for Narrowband Interference Suppression in Spread Spectrum Communications", *IEEE Trans. Commun.*, Vol. 43, pp. 1725-1737, 1995.
8. J.H. Winters, J. Salz, and R.D. Gitlin, "The Impact of Antenna Diversity on the Capacity of Wireless Communications Systems", *IEEE Trans. Commun.*, Vol. 42, pp. 1740-1751, 1994.
9. A.F. Naguib and A. Paulraj, "Performance of CDMA Cellular Networks with Base-Station Antenna Arrays", in *Mobile Communications: Advanced Systems and Components*, 1994 International Zurich Seminar on Digital Communications Proceedings, Zurich, Switzerland, pp. 87-100, 1994.
10. Y. Yoon, R. Kohno and H. Imai, "A Spread-Spectrum Multiaccess System with Cochannel Interference for Multipath Fading Channels", *IEEE Journal on Selected Areas in Communications*, Vol. 11, pp. 1067-1075, 1993.
11. X. Wu and A. Haimovich, "Space-Time Optimum Combining for CDMA Communications", The special Issue on "Signal Separation and Interference Cancellation for Personal, Indoor and Mobile Radio Communications (PIMRC)" *Wireless Personal Communications*, Vol. 3, pp. 73-89, 1996.
12. A. Shah and A.M. Haimovich, "Space-Time Optimum Combining for CDMA Overlay for Personal Communication Systems", *Wireless Personal Communications*, 1996. Accepted for publication.
13. V. Bogachev and I. Kiselev, "Optimum Combining of Signals in Space-Diversity Reception", *Telecommun. Radio Eng.*, Vol. 34/35, pp. 83-85, 1980.
14. S. Haykin, *Adaptive Filter Theory*, Prentice Hall: Englewood Cliffs, NJ, third ed., 1996.
15. D. Slepian and H.O. Pollak, "Prolate Spheroidal Wave Functions Fourier Analysis and Uncertainty - III: The Dimension of the Space of Essentially Time- and Band-Limited Signals", *The Bell System Technical Journal*, pp. 1295-1336, 1962.
16. J. Proakis, *Digital Communications 3/e*, McGraw-Hill: New York, 1995.
17. J. DiFranco and W. Rubin, *Radar Detection*, Prentice Hall: Englewood Cliffs, NJ, 1968.
18. M. Abramowitz and I.A. Stegun, *Handbook of Mathematical Functions* (tenth printing), National Bureau of Standards: Washington, DC, 1972.

19. J. Seaborn, *Hypergeometric Functions and Their Applications*, Springer-Verlag: New York, 1991.
20. H. Exton, *Handbook of Hypergeometric Integrals*, Ellis Horwood Limited: Chichester, UK, 1978.



Alexander M. Haimovich received the B.Sc. degree in electrical engineering from the Technion Institute of Technology, Haifa, Israel in 1977. He received the M.Sc. degree in electrical engineering from Drexel University in 1983, and the Ph.D. degree in systems from the University of Pennsylvania in 1989.

From 1983 to 1987 he was a Senior Engineer with American Electronic Laboratories in Lansdale, PA. From 1987 to 1989 he was an Assistant Professor at the New Jersey Institute of Technology. He was Senior Staff Consultant at American Electronic Laboratories from 1989 to 1990. From 1990 to 1992 he was Chief Scientist at JJM Systems in Warminster, PA. He is currently Associate Professor at the New Jersey Institute of Technology. His research interests include adaptive array processing for radar and wireless communications.



Amit Shah received the B.S. and Ph.D. degrees in electrical engineering from New Jersey Institute of Technology, Newark, NJ, U.S.A., in 1992 and 1997, respectively. He is currently a member of the technical staff at Lucent Technologies, Whippany, NJ. Prior to joining Lucent Technologies, he was a research assistant at New Jersey Institute of Technology. His research interests include adaptive array processing for wireless communications.